Surface Modification of High Carbon Steel by Autogenous Pulsed Tungsten Inert Gas Arcing

Somnath Basu*, P. K. Ghosh*, J. S. Saini****

* Professor & Dean , IIT,Roorkee, India, e-mail : prakgfmtiitr@gmail.com

** Professor, DIT University, Dehradun,India

*** Research Scholar at Uttarakhand Technical University, Dehradun, India

ABSTRACT

Pulsed Tungsten Inert gas arcing (PTIGA) has been employed at various pulse parameters keeping the energy input constant for surface modification of high carbon steel (En-31) by controlled fusion. Analytical studies on thermal cycle and isotherm of fused surface have been carried out to predict microstructure of the fusion and heat affected zones. The analytical predictions have been verified by the experimental observations of modified surface characteristics. The ability of PTIGA process to control the energy input and its distribution significantly influences the solidification behavior, nature of phase transformation and morphology of various phases in the matrix. It happens due to influence of arcing over the depth of fusion and cooling characteristics of matrix during solidification. Optimization of pulse parameters of the PTIGA process allows surface modification of En-31 steel plate with significantly improved hardness avoiding hot crackin

Keywords : Pulsed TIG arcing, high carbon steel, controlled fusion, thermal characteristics, microstructure, hardness.

1.0 INTRODUCTION

Requirement of special surface properties like hardness of a rather conventional material to serve the specific requirements of various service conditions, has been found as a crucial need in many advanced technologies. In order to address this requirement several methods are there in practice that includes modification of physical, chemical, mechanical and metallurgical characteristics of the surface of a metallic substrate. In order to serve this purpose medium to high carbon steels are often used with surface modification commonly made by mechanical working, cryogenic heat treatment, and fusion of the substrate as well as extra deposition on it [1-5]. Various treatments have their limitations in application depending upon, cleanliness, versatility and extent of their influence on the substrate as function of depth of modification and type of control over the morphology and surface chemistry. In this context the surface fusion of a metallic substrate by tungsten inert gas arcing has been found [6] quite effective to produce desired surface modification of metallic substrate in reference to phase transformation up to a significant depth required for engineering applications of wear and friction. However, the high carbon content makes the steel more susceptible to hot cracking in fused zone [15]. The control of such susceptibility to cracking is generally addressed by favorable regulation of solidification mechanism. During conventional arc welding the unnecessary high heat input is normally avoided to eliminate hot cracking in weld pool. Use of interrupted heat input by introducing pulsed current in arc welding significantly influences the solidification mechanism of fused metal. Thus, an appropriate control of pulsed current process may be helpful to reduce its hot cracking susceptibility.

The use of pulse current during surface fusion by tungsten inert gas (TIG) arcing is more beneficial to control the transformation behavior more effectively due to precise control of thermal distribution in the arcing system [9]. Pulse TIG (PTIG) is better than conventional TIG because it can operate at a relatively higher energy input of high current but maintains a relatively low net heating of the base metal primarily due to

interruption in arcing causing interrupted fusion and solidification of base metal. It allows greater control of heating with comparatively larger fusion and deeper penetration at faster speed of arc movement. PTIG has ability to control energy input as well as its distribution in the process that significantly influences the solidification behavior, nature of phase transformation in the matrix through its influence over depth of fusion and cooling characteristics of matrix during solidification. Thus, the use of pulse TIG arcing process can be further explored for surface modification of alloys having relatively complex behavior of phase transformation that requires precise control of isotherm and thermal cycle of fused and heat affected zones. It may result improved quality of thermally modified zone especially with respect to its microstructure. However the control of pulse current process is quite complicated due to involvement of its simultaneously interacting parameters like peak current (I_p),base current (I_b), pulse frequency (f), peak current duration (t_p) and base current duration (t_b). But such difficulties are amicably addressed by control of pulsed current process through a hypothetically derived dimensionless factor ϕ which has been successfully used in case of the metal inert gas (MIG) welding and tungsten inert gas (TIG) arcing processes [9,10]. The dimension less parameter is expressed as equation (1):

$$\phi = (I_b / I_p) f t_b \quad \ldots\ldots\ldots\ldots\ldots \quad (1)$$

In view of the above, an effort has been made to study the surface hardening of relatively high carbon En-31 grade steel which is a commonly used material for bearings and grinding media balls where high hardness and wear properties with relatively tougher core are important. Considering the scope for hardening of this material by heat treatment process optimization of pulse parameters has been studied that can be used for surface modification of high carbon En -31 steel using pulse TIG arcing (PTIGA) process to enhance its hardness maintaining a relatively tougher core. Analytical studies on heat flow in surface fusion have been carried out to draw isothermal and thermal cycle plots for various pulsed current arcing parameters affecting the transformation in fused zone. Subsequently micro structural analysis and corresponding changes in hardness have been studied in order to optimize the pulse parameters to get desired hardness of surface modification by PTIGA process.

2.0 EXPERIMENTAL WORK

Surface modification of En -31- high carbon steel, having typical physical properties and chemical compositions as given in **Tables – I** and **II** respectively, was carried out using TIG arcing generated from a 'Fronius' Magicwave 1700 pulsed TIG welding Machine. A 3.2 mm diameter non consumable thoriated tungsten electrode was used to strike an arc in DCEN mode between the electrode and the work piece under commercial argon gas shielding environment flowing at a rate of 18 L/min. The surface modification by fusion of base material was carried out on a coupon size of 150x75x5 mm. Prior to fusion by arcing the substrate surface was mechanically cleaned by rubbing with the emery paper followed by wiping with acetone in order to make it free from contaminations such as rust and grease. Surface modification of the substrate was carried out by using PTIGA process with pulse frequencies (f) of 0.5,1,2 and 4 Hz. The pulse frequencies were selected based on an earlier work reported [9] in this area and the thermal pulsing frequency suggested in 'Fronius' machine manual. The PTIGA was carried with parameters as noted in **Table –III**. The arc voltage (V) and torch travel speed (S) was kept practically constant as 11 V, 9 cm/min. Duty cycle was varied from 30% to 70%. Arcing was carried out at a given heat input of 7.04±0.94 kJ/cm estimated by [(ηxAxV)/S] where, the system efficiency η has been considered as 0.75 [7]. The given range of heat input was maintained by adjustment of welding speed (S). Expression for estimation mean current (Im) is given in equation (2). During experimental work the voltage fluctuation noted at machine output display terminal was less than ± 10% while current fluctuation was less than ± 0.25%. Surface modification by controlled fusion was carried out on the base plate at ambient temperature by single pass arcing procedure as typically shown (**Fig. 1**).

$$I_m = [(I_p t_p + I_b t_b)/ (t_p + t_b)] \quad \ldots\ldots\ldots\ldots\ldots \quad (2)$$

Table I Physical properties of the base material

Material	Density (kg/m^3)	Melting Point (^0C)	Thermal Conductivity ($Wm^{-1}.K^{-1}$)	Sp. heat (Cp) (J/kg K)
EN-31 Steel	7810	1200	46.6	0.0452

Table-II : Chemical composition of base material

Material	Chemical composition (Wt.%)						
	C	Mn	Si	S	P	Cr	Fe
EN31 Steel	0.92	0.58	0.30	0.024	0.020	1.48	Remainder

Table-III : Pulse current TIG arcing parameters for En-31

IP (A)	Ib (A)	f (Hz)	Duty cycle (%)	tp (ms)	tb (ms)	im (A)	ϕ
170	86	0.5	30	600	1400	111	0.35
			50	1000	1000	128	0.25
			70	1400	600	145	0.15
	1.0		30	300	700	111	0.35
			50	500	500	128	0.25
			70	700	300	145	0.15
	2		30	150	350	111	0.35
			50	250	250	128	0.25
			70	350	150	145	0.15
	4		30	75	175	111	0.35
			50	125	125	128	0.25
			70	175	75	145	0.15

The surface characteristics of each modified sample were studied on the samples machined out from a distance more than 12 mm from the arc initiation point along the arc travel line in order to ensure the stable temperature zone of fusion. Metallographic studies were carried out on the transverse section to the arc travel line. The specimens were prepared by standard metallographic procedure of polishing with emery papers of different grit sizes followed by final polishing with diamond paste. Optical microscopic studies were carried out on the specimen after 2% Nital etching. Vickers pyramid hardness (HV) was measured on the polished surface transverse to arc travel line by indentation at 10 kgf force with 15 sec dwell time.

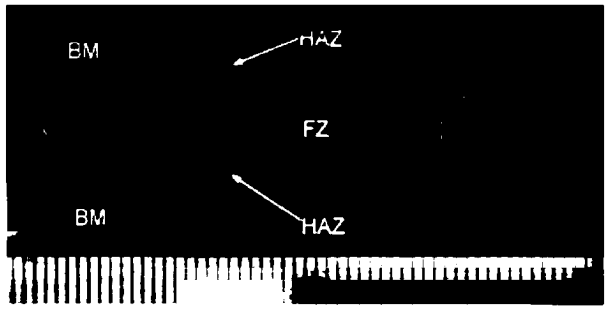

Fig.1 Typical surface zones at single pass arcing ;[Scale in mm].

3.0 THERMAL ANALYSIS OF FUSION

The increase in initial temperature T_0 at t = 0 to temperature T after t = t of a semi infinite plate with a double ellipsoidal heat source moving at a velocity v is expressed [8] in equations (3) to (7).

$$T-T_0 = \frac{3\sqrt{3}Q_d}{2pcP\pi}\int_0^t \frac{dt'}{\sqrt{\{12a(t-t')+a_h^2\}\{12a(t-t')b_h^2\}}} X\left\{\frac{A'}{\sqrt{12a(t-t')+c_{hf}^2}} + \frac{B'}{\sqrt{12a(t-t')+c_{hb}^2}}\right\} \quad \text{..... (3)}$$

$$\text{where, } A' = r_f \exp\left\{\frac{3(x-vt)^2}{12a(t-t')+c_{hf}^2} - \frac{3y^2}{12a(t-t')+a_h^2} - \frac{3z^2}{12a(t-t')+b_h^2}\right\} \quad \text{..... (4)}$$

$$A' = r_f \exp\left\{\frac{3(x-vt')^2}{12a(t-t')+c_{hb}^2} - \frac{3y^2}{12a(t-t')+a_h^2} - \frac{3z^2}{12a(t-t')+b_h^2}\right\} \quad \text{..... (5)}$$

Front and back proportion coefficients are

$$r_f = \frac{2c_{hf}}{c_{hf}+c_{hb}} \quad \text{..... (6)}$$

$$\text{and } r_b = \frac{2c_{hb}}{c_{hf}+c_{hb}} \quad \text{..... (7)}$$

Q_d is heat transferred per unit time for distributed heat source, ρ is mass density of base metal, c is specific heat of base metal, a is thermal diffusivity of base metal and a_h, b_h, c_{hf}, and c_{hb} are the double ellipsoidal heat source parameters defined by a location having at least a power density of 5% to that of the centre on surface of the ellipsoid **(Fig. 2)** [10]. It is considered [8] as $c_{hf} = a_h$ and $c_{hb} = 2c_{hf}$. Thus, a_h and b_h are the only two parameters which are to be selected by comparing the best fit value of the width and penetration of fusion zone respectively with their corresponding values estimated on the assumed values of a_h and b_h.

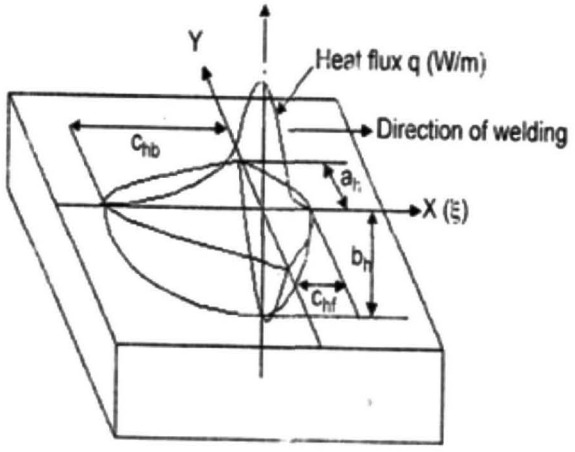

Fig. 2 : Schematic diagram of double ellipsoidal heat source

With this estimation and using the data as given in **Table –I** and **III** an analytical model was developed for estimation of temperatures at different points at different times with heat input of 7.04 kJ/cm. Based on this understanding isothermal curves (**Fig. 3**) and thermal cycle of FZ and HAZ (**Fig. 4**) of En-31 steel at the heat input of 7.04 kJ/cm were drawn.

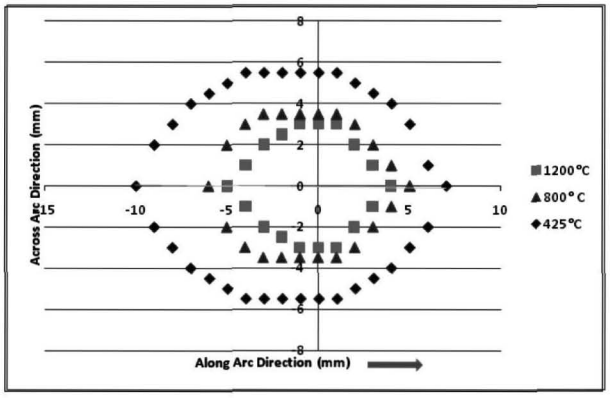

Fig. 3 : Isothermal curves of PTIG arcing on surface of the steel plate

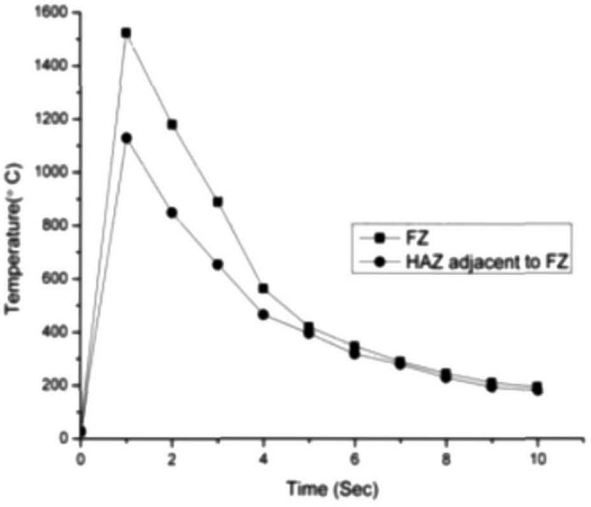

Fig. 4 : Thermal cycle of FZ and HAZ at 4 mm from FZ centre line of the steel plate.

4.0 RESULTS AND DISCUSSIONS

4.1 **Surface appearance of fused zone :** Surface appearance of the fused zone was thoroughly studied with respect to ripple formations and surface integrity representing the solidification behavior at different f and ϕ values. Some typical photographs of the ripple formation as a function of pulse parameters are shown in **Fig. 5**. It appears that f and ϕ have appreciable effect on ripple pattern and number of

ripples per unit length which indicates the coarsening of ripple that in turn broadly indicates the cooling characteristics of the fused surface. At pulse frequencies of 0.5, 1, 2 and 4 Hz the effect of ϕ on ripple concentration per unit length of fusion modified surface has been shown in **Fig. 6**. The figure shows that at a given ϕ the decrease of pulse frequency increases number of ripples per unit length **(Fig. 5 (a))** and at a given pulse frequency the increase of ϕ significantly enhances the same by making it appreciably finer **(Fig. 5 (b))**. Considering **Fig. 4** it appears that FZ has temperature much higher than the melting point of base material. At higher frequency the available time (t_b) for cooling of the super heated fused zone is relatively less and IP can be restored before solidification starts in fused base metal this may be primarily attributed to relatively less number of ripple formation ion the solidified matrix as observed in **Fig. 5 (a)**. Transverse section of the modified surface by fusion clearly shows (**Fig. 7**) the typical profile of the fused zone (FZ) and heat affected zone (HAZ) in base metal (BM).

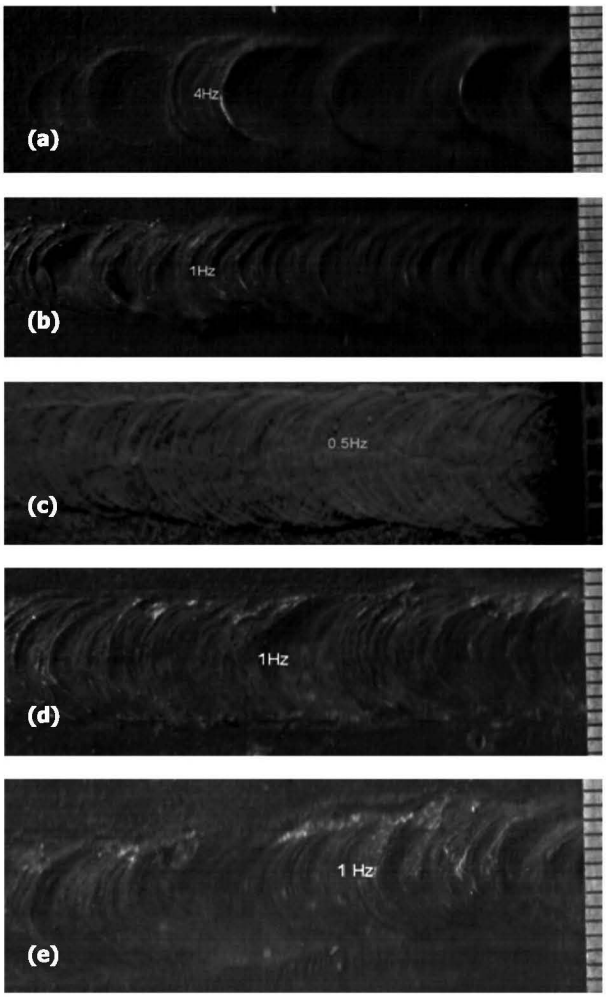

Fig. 5 : Typical appearance of variation in ripple formation on the fused surface of base plate as a function of pulse frequency (f) at a given ϕ = 0.15 (a) 4 Hz (b) 1Hz (c) 0.5 Hz and as a function of ϕ at a given f = 1 Hz (d) ϕ = 0.15 and (e) ϕ = 0.25 ; [Scale in mm]

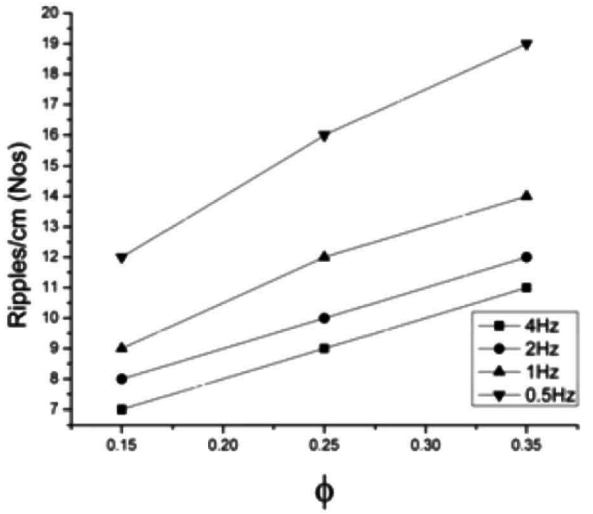

Fig. 6 : At a given heat input 7.04±0.94 kJ/cm effect of pulse frequency and ϕ on ripple concentration per unit length of fused surface of the base plate.

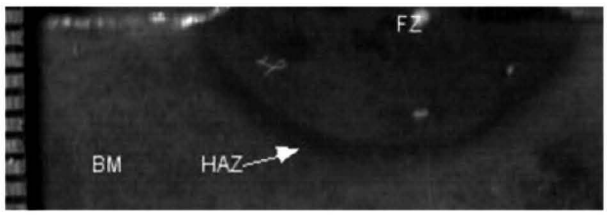

Fig. 7 : Typical appearance of transverse section of surface modification by PTIG arcing ; [Scale in mm].

4.2 **Thermal and solidification behavior of fused zone:** The thoroughly studied surface appearance of fused zone with respect to ripple formation at different parameters of PTIGA process has been used to estimate the cooling rate and growth rate using ripple concentration per unit length of the fused zone in the line of a successful analysis reported earlier [9,11]. The geometric approach of the analysis of ripple characteristics has been schematically shown in **Fig. 8**. The analytical expressions used for estimation of cooling rate and the resulting characteristic features of solidification of the fused zone primarily with respect to the growth rate of primary solid are shown in equations (8) to (12).

Ripple lag ratio (R_{lg}) = L_{rg} / W_{rg} .....(8)

Growth Rate (R_G) = S cos α .....(9)

Solidification temperature gradient (G) = T_m/X_{hw} ..... (10)

Cooling Rate (C_R) = GR_G θ ..... (11)

θ = $\tan^{-1}$ (W_{rg} / 2 L_{rg}) ..... (12)

Where, L_{rg} is length of ripple lag, W_{rg} is width of molten pool, T_m is melting temperature of base plate and X_{hw} is distance between heat source and rear of the weld pool. All quantitative measurements on the fused surfaces were performed with Adobe Photoshop 7 applied on fused zone photographs captured in computer.

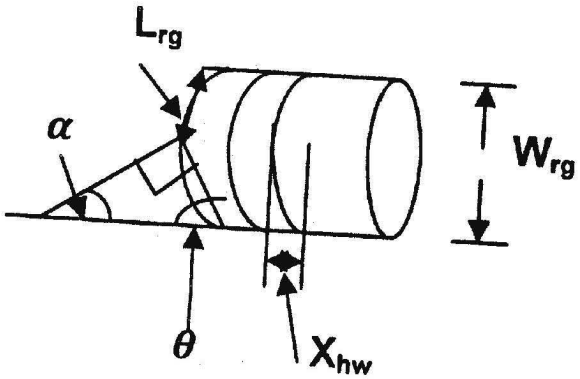

Fig. 8 : Schematic diagram showing the characteristic features of ripples on fused surface.

The effect of ϕ on cooling rate of the fused zone during arcing at different pulse frequencies of 0.5, 1, 2 and 4 Hz has been shown in **Fig. 9**. Similarly the effect of ϕ on growth rate of the primary solid in the fused zone during arcing at different pulse frequencies of 0.5, 1, 2 and 4 Hz has been shown in **Fig. 10**. The figures show that at a given pulse frequency the increase of ϕ significantly increases the cooling rate as well as primary solid growth rate while they significantly reduce with the increase of pulse frequency at a given ϕ. The relatively low cooling rate at higher pulse frequency may have primarily happened due to occurrence of more frequent IP which results in to more frequent heat input that reduces the temperature gradient of fusion zone to its relatively large area of wide spread hot surrounding heat sink. The predomination of the ability of heat extraction from the fused zone based on thermal gradient between the location of arcing and its surroundings may gradually become more active at lower frequency of arcing due to availability of more time for heat dissipation in between successive pulses creating a relatively shorter hot surrounding and a closer relatively active heat sink. At a given pulse frequency the increase of cooling rate with the increase of ϕ may have happened due to less heat buildup in fused pool [9] that keeps the surrounding heat sink more active. The earlier observation [11] has explained the reason for change in heat buildup as a function of ϕ primarily due to interruption in fused metal deposition in case of metal inert gas (MIG) welding. In the same line of understanding of the effect of interruption in arcing the solidification behavior of melt in PTIG process may be understood for its thermal balance. The variation in heat buildup is a function of ϕ due to change in pattern of interruption of arcing influencing the repetitive process of fusion, partial solidification of melt, appropriate re melting of primary solids that varies the thermal balance of the fusion zone. However, in **Fig. 9** it is found that at the low pulse frequency of 0.5 Hz the rate of increase of cooling rate with the increase of ϕ is relatively higher than that observed in case of higher pulse frequencies. This may be understood by considering the competitive aspect of heat buildup as function of ϕ and available scope of heat dissipation at low pulse frequency. The cooling rate at 0.5 Hz varies from 315 °C/sec at ϕ = 0.25 to 485 °C/sec at ϕ = 0.4, whereas the corresponding values at 4 Hz are 207 °C/sec and 289°C/sec respectively. The increase of primary solid growth rate as a function of ϕ and pulse frequency can be realized in concurrence with the behavior of cooling rate. A higher cooling rate and growth rate of primary solid promotes formation of comparatively finer matrix morphology in the fused zone.

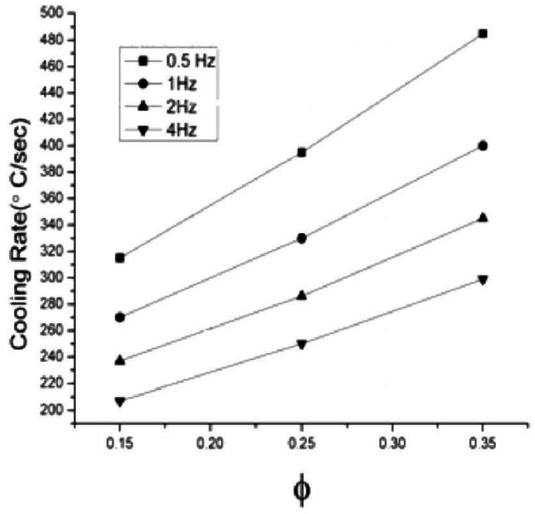

Fig. 9 : At a given heat input in put 7.04±0.94 kJ/cm effect of ϕ on cooling rate estimated from appearance of ripples on fused surface during arcing at different pulse frequencies.

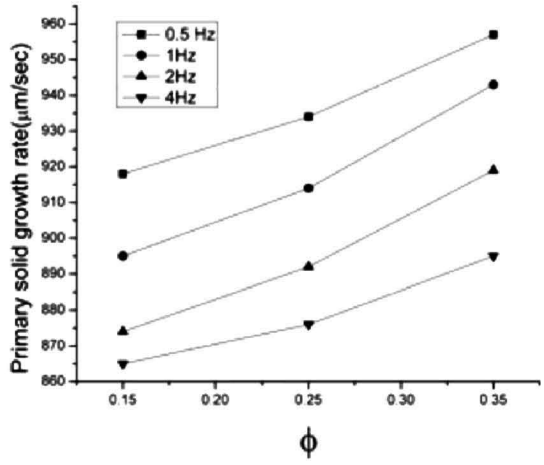

Fig. 10 : At a given heat input 7.04±0.94 kJ/cm effect of ϕ on primary solid growth rate estimated from appearance of ripples on fused surface during arcing at different pulse frequencies.

4.3 **Geometry of modified zone:** At a given heat input of 7.04±0.94 kJ/cm the effect of ϕ on the width and depth of penetration of the fusion zone observed during pulsed arcing at 0.5, 1, 2 and 4 Hz are shown in **Figs. 11** and **12** respectively. The figures show that in general at a given heat input the increase of ϕ at a given f and the increase of f at a given ϕ significantly reduces the width and depth of penetration of the fusion zone. The width of measured fusion zone lies in the range of about 6.5 to 9.4 mm as a function of ϕ and f. This is interesting to note that at a given heat input the geometry of fusion zone can be manipulated by changing the pulse parameters of TIG arcing. This may effectively influence the isotherm, thermal cycle and consequently the solidification behavior of the fusion zone affecting its microstructure. The minimum fusion width as 6.5 mm is found at f = 4 Hz and ϕ = 0.35 while its maximum value of 9.4 mm is noted at f = 0.5 Hz and ϕ = 0.15. Similarly the depth of penetration of fusion as a function of the ϕ and f has been found to be maximum of about 4.1 mm at f = 4 Hz and ϕ = 0.15 while it is noted to be lowest as about 2.6 mm at f = 0.5 Hz and ϕ = 0.35.

Effect of pulse parameters (ϕ and f) on the geometry of fused zone as revealed in its transverse section has been shown in **Fig. 13**. At different pulse frequencies the variation of width to depth ratio of fusion zone as a function of ϕ has been shown in **Fig. 14**. The figure depicts that keeping the pulse frequency and ϕ at 4 Hz and 0.15 respectively gives lowest ratio of 1.78, while the maximum ratio of 3.3 is obtained at the pulse frequency and ϕ of 0.5 Hz and 0.35 respectively. A larger width of fusion zone introduces faster heat loss by convection and radiation while a higher depth of fusion at its given width enhances the area of contact with the base metal and consequently gives faster conduction heat loss. However a larger width of fusion distributes heat in larger surface area of the base plate and hence enhances its cooling rate.

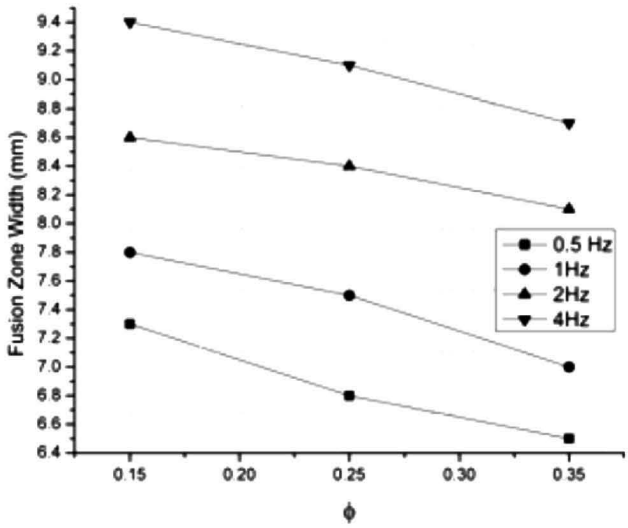

Fig. 11. : At a given heat input 7.04±0.94kJ/cm the effect of ϕ on the measured width of fusion zone during arcing at different pulse frequencies.

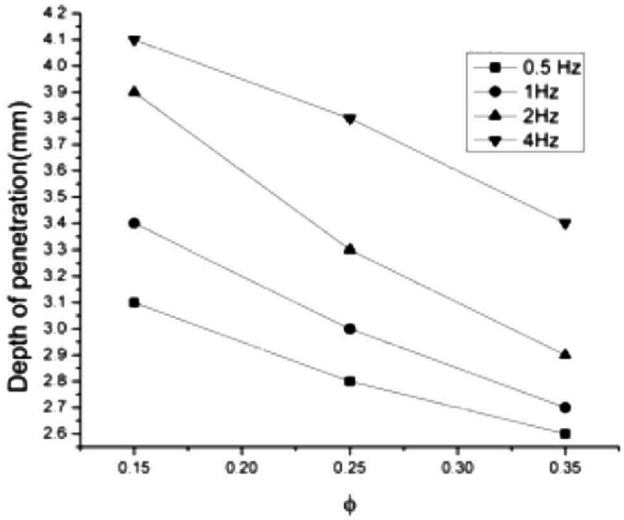

Fig. 12 : At a given heat input 7.04±0.94kJ/cm the effect of ϕ on the measured depth of penetration during arcing at different pulse frequencies.

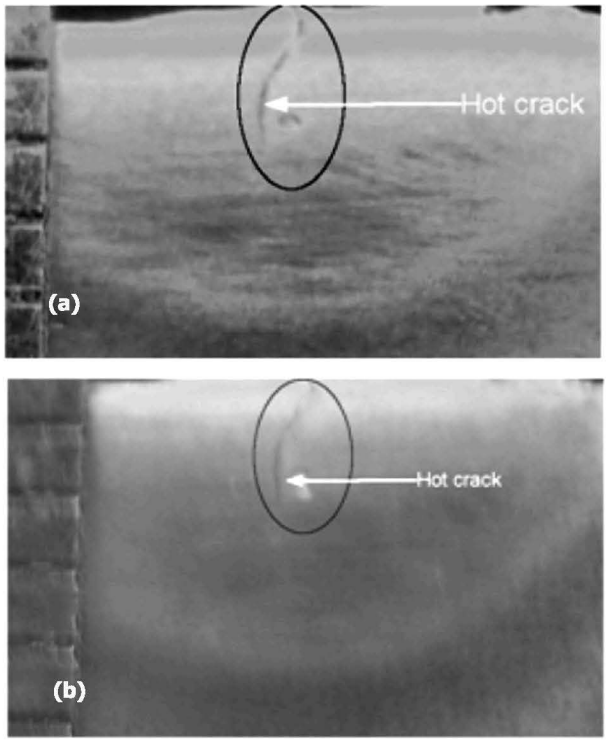

Fig. 13 Typical transverse section of the fused zone at (a) f=0.5 Hz and ϕ= .0.15 and (b) f=1 Hz and ϕ=0.5 ; [Scale in mm].

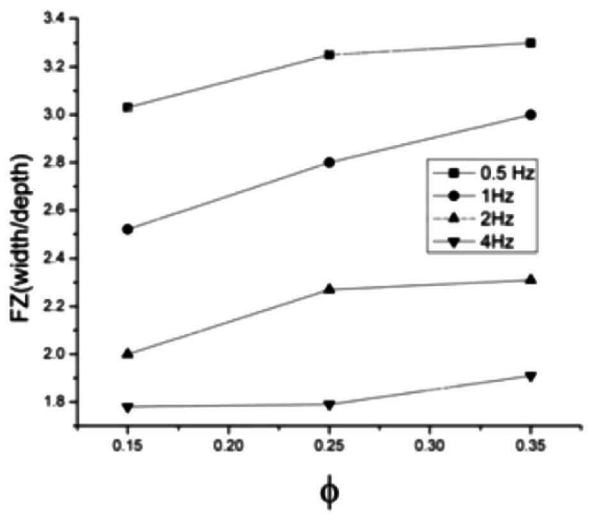

Fig. 14 : At a given heat input 7.04±0.94kJ/cm width to depth ratio of fusion zone at different PTIGA parameters.

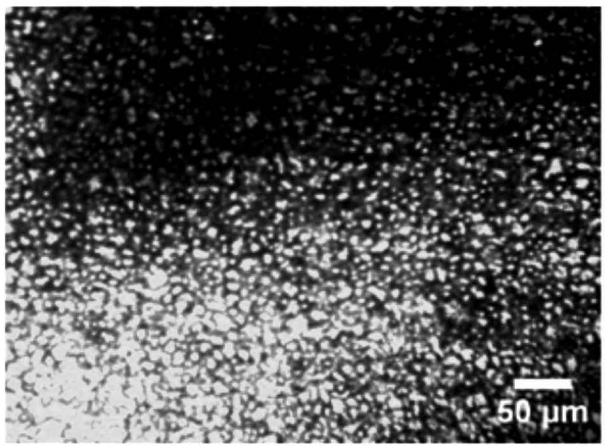

Fig. 15 : Typical microstructure of base metal

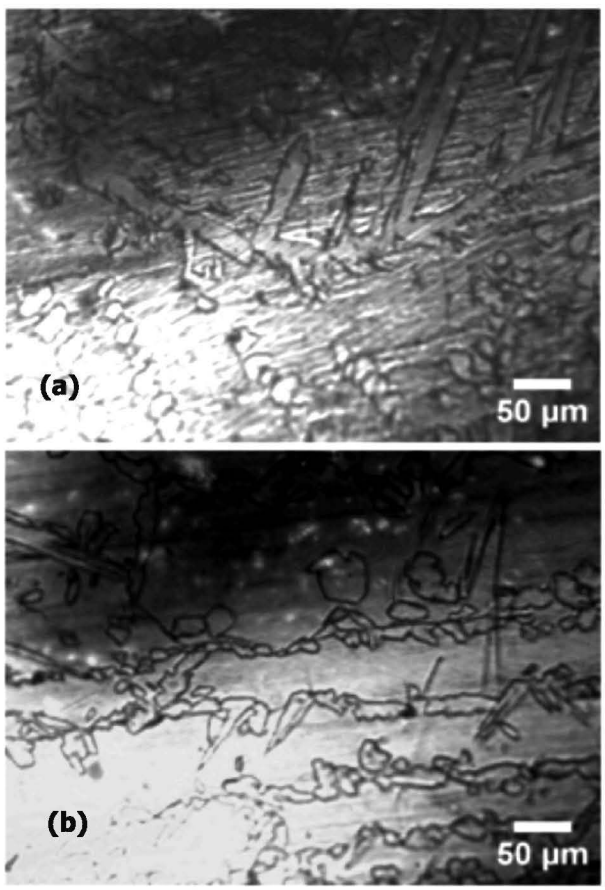

Fig. 16 : Change in microstructure of FZ as a function of pulse frequency at given ϕ=0.35 and (a) 0.5 Hz and (b) 4 Hz.

4.4 Microstructure : Typical microstructure of the base metal has been shown in **Fig. 15**. The figure shows that the matrix consists of evenly dispersed fine grain pearlite and cementite phases this is in agreement with Fe-C diagram for hyper eutectoid steel and [12].

At a given ϕ of 0.35 the effect of pulse frequencies of 0.5 and 4 Hz on the microstructure of fusion zone has been shown in **Fig. 16 (a)** and **(b)** respectively. The microstructures show that the matrix is having significant dendritic growth at low pulse frequency of 0.5 Hz but its presence is practically

insignificant at relatively higher pulse frequency of 4 Hz. The comparatively less growth of dendrite in the fusion zone of higher pulse frequency is primarily attributed to more effective interruption in solidification under the pulsed current [13]. At the given ϕ of 0.35 the corresponding microstructure of HAZ of base metal adjacent to the fusion zone observed in case of the PTIG arcing at the pulse frequencies of 0.5 and 4 Hz has been shown in **Fig. 17 (a)** and **(b)** respectively. The micro-structures show the presence of martensite, alloy carbides and retained austenite. The martensite is plate type [14].

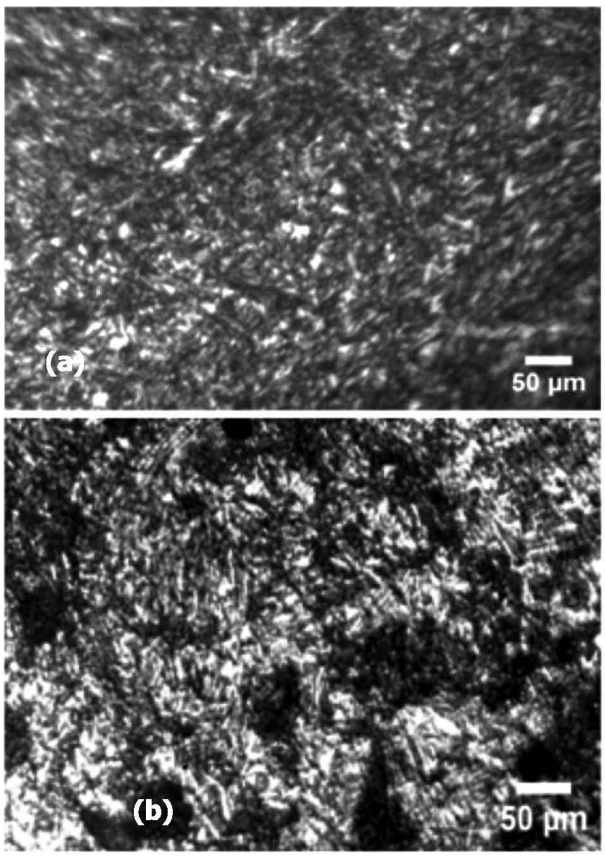

Fig.17 : Change in microstructure of HAZ as a function of pulse frequency at given ϕ=0.35 (a) 0.5 Hz and (b) 4 Hz.

4.5 Hardness : In the line of variation of microstructure of fusion zone and HAZ of base metal adjacent to FZ as a function of ϕ and pulse frequency their hardness was also varied. The surface treatment by using the PTIGA process at any pulse parameters has always been found to increase the matrix hardness from that of the base metal measured as 180 ± 6HV. The nature of variation of average hardness of the fused zone and the HAZ of base metal adjacent to the FZ as a function of ϕ at different pulse frequencies of 0.5, 1 ,2 and 4 HZ has been shown in **Figs. 18 (a), (b),(c)** and **(d)** respectively. The figures show that at any pulse frequency the increase of ϕ from 0.15 to 0.35 significantly increases the hardness of both the FZ and HAZ. It is observed that at a given ϕ the increase of pulse frequency relatively increases the hardness of FZ as well as HAZ. At a given pulse frequency the increase of hardness of the FZ with the increase of ϕ is in agreement to their cooling rate **(Fig. 9)** and microstructure as discussed above. The maximum rise of average hardness of FZ has been found of the order of 415 HV during arcing at the ϕ and pulse frequency of 0.35 and 4 Hz respectively which is about 130% higher than that of the base metal. Similarly the hardness of HAZ has been found to be raised up to about 292 HV which is also about 62% higher than that of the base metal.

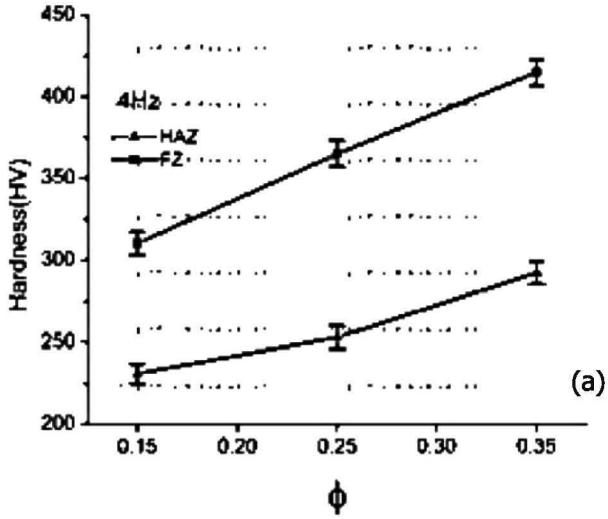

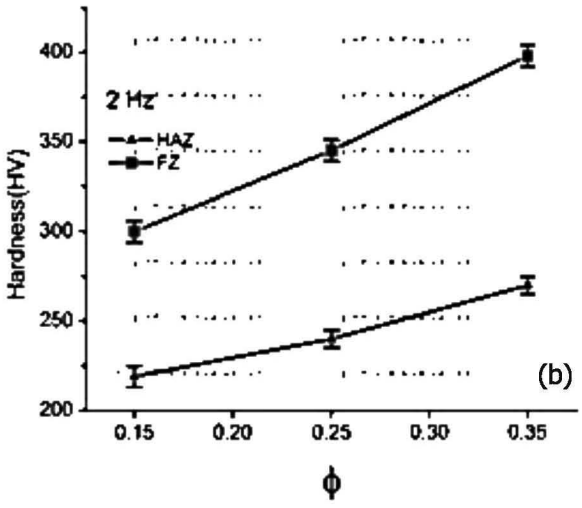

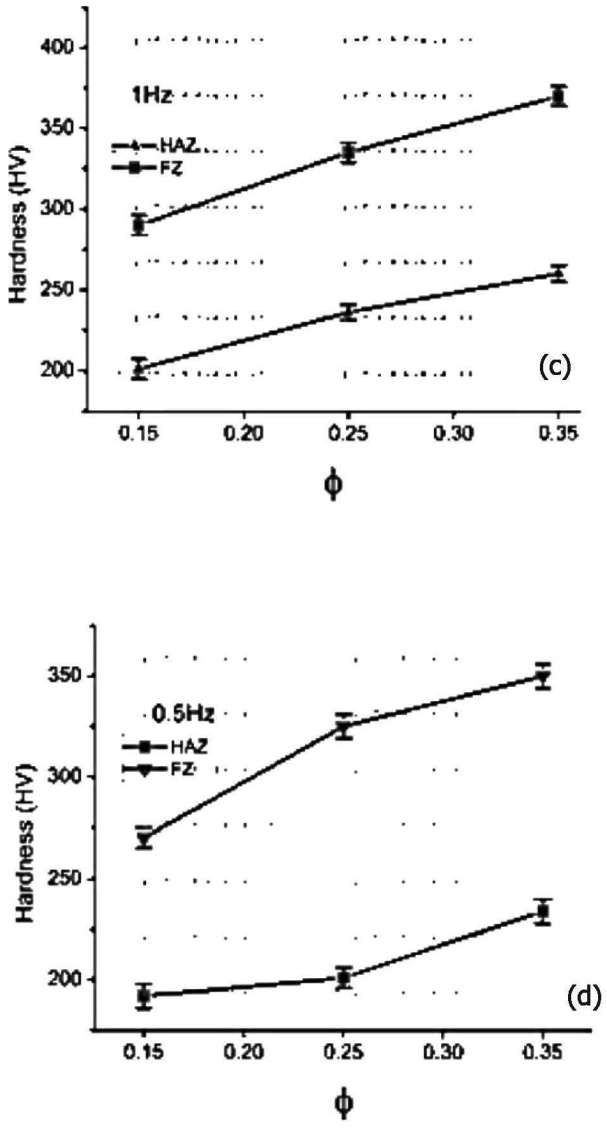

Fig.18 : Hardness at FZ and HAZ at pulse frequencies (a) 4Hz (b) 2Hz (c) 1Hz (d) 0.5 Hz

4.6 Hot cracking: The cracking index (UCS), expressed as equation(13) [15], for the susceptibility to solidification cracking or hot cracking of the high carbon En-31 steel is estimated as 210 which is much higher than the recommended limiting value as 25 for avoiding the cracking. The high susceptibility of this steel to hot cracking is clearly noted during its surface fusion at various parameters of the PTIGA process as shown in **Fig. 19.** At same parameter cracks at transverse section to the arc travel line is shown in **Fig. 20.** However, the high cracking susceptibility of this steel can be reduced by controlling the geometry of the fused zone at a given heat input as well as sulphur and phosphorus content [16].

$$U_{cs} = 230C + 190S + 75P + 45Nb - 12.3Si - 5.4Mn - 1 \quad \ldots\ldots (13)$$

Where, the elements are considered as wt.%.

In the line of earlier discussions on the process of heat dissipation from the fusion zone, a parameter of its width to depth ratio may be considered as a measure to understand the characteristics of cooling rate of this location that significantly influences the phase transformation and development of stresses in this region. A slow cooling of fused zone can make it susceptible to hot cracking when a higher cooling rate may enhance hard phase transformation like martensite and develop higher stress in the matrix that can promote cold cracking. Lower width to depth ratios can be attributed as a reason for hot crack at higher frequencies.

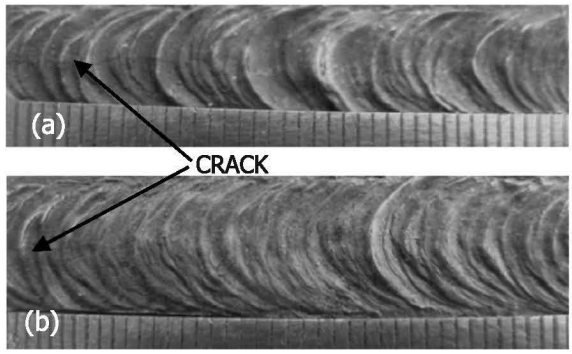

Fig. 19 : Typical Hot cracks at fused zone surface of En-31 (a) f=2Hz and ϕ= .15 (b) f=4Hz and ϕ = .25

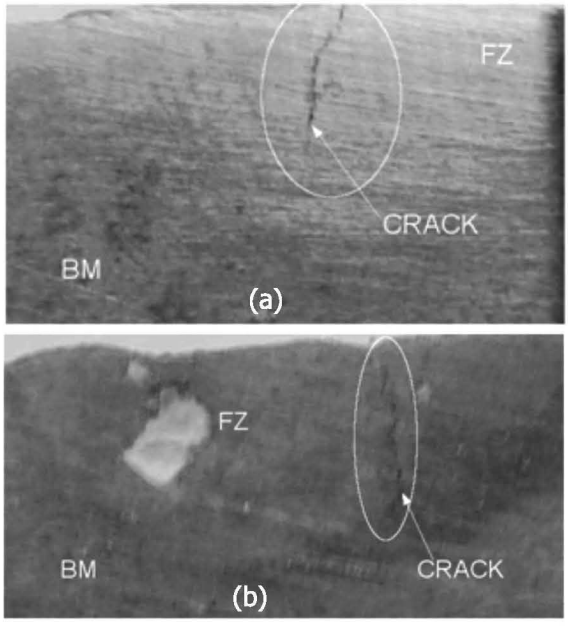

Fig. 20 : Typical hot cracks at surface transverse to fused zone of En-31 at (a) f=2Hz, ϕ= .15 and (b) f=4Hz, ϕ = .25

Surface integrity in the experimental parameter range was poor. Other than 0.5 Hz at ϕ = .35 all the fused surfaces were having hot cracks as typically shown in **Fig. 6**.

5.0 CONCLUSION

It has been observed that En-31 steel surface can be modified by PTIG Arcing. Hardness value can be raised up to 415 HV in FZ and 292 in HAZ area. But at such cases hot cracks are developed. The extent of fusion and its thermal behavior and consequently its characteristics of solidification and phase transformation can be manipulated by changing the pulse frequency and ϕ that takes care also of other pulse parameters as their summarized influence. So optimum hardness without surface crack was found to be 350 HV at FZ and 234 at HAZ at f = 0.5 Hz and ϕ = .35 at 2.1 mm depth. The morphology of entire modified base material is controlled by thermal cycle which consists of heating rate, peak temperature, cooling rate and pulse on /off duration. There is scope for detailed study of these aspects to achieve a desired phase transformation at a relatively higher cooling rate under a active heat sink in a localized heating zone.

REFERENCES

(1) A. Bhattacharya, A. Batish and G. Singh (2011); Surface Modification of High Carbon High Chromium, EN31 and Hot Die Steel Using Powder Mixed EDM Process, Materials Science Forum, Vol. 701, pp 43-59 .

(2) X. M. Zhang, H. C. Man and H. D. Li (1997); Wear and friction properties of laser surface hardened EN31 steel, Journal of Materials Processing Technology, Vol. 69. (1-3), pp162-166.

(3) A. S. C. M. D'Oliveira, R. S. C. Paredes and R. L. C. Santos (2006); Pulsed current plasma transferred arc hardfacing, Journal of Materials Processing Technology, Vol.171(2), pp167-174

(4) R. Singh and J. F. Gerald(1997); Surface composites : A new class of engineered materials, Journal of Materials Research, Vol.12, (3), pp769-773.

(5) S. Harish, A. Bensley, D. M. Lal, G. B. Lenkey and A. Rajadurai (2009); Microstructural Study of Cryogenically treated En-31 bearing steel, Journal of Materials Processing Technology,Vol. 209, (7), pp3351-3357.

(6) A U Orlowicz and A.Trytek (2005), Use of the GTAW method for surface hardening of cast iron, Welding international research supplement, Vol.19 (5), pp341-348.

(7) K. Poorhaydari, B. M Patchett and D. G. Ivey (2005); Estimation of cooling rate in the welding of plates with intermediate thickness, Welding Research, (Oct), pp 149-s-155-s.

(8) N. T. Nguyen, A. Ohta, K. Matsuoka, N. Suzuki and Y. Maeda (1999), Analytical Solutions for Transient Temperature of Semi-Infinite Body Subjected to 3-D Moving Heat Sources" "Welding Research, (Aug), pp266-s-274-s.E

(9) P. K. Ghosh and Ravindra Kumar (2015); Surface modification of Micro-Alloyed High-Strength Low-Alloy Steel by controlled TIG Arcing Process, Metallurgical and Materials Transaction A, Vol.46(2), pp 831-842.

(10) V. K. Goyal (2007); Effect of thermal and solidification behavior on characteristics of pulsed current GMA weld, Ph.D thesis submitted at IIT, Roorkee, India.

(11) P.K.Ghosh, V.K.Goyal, H.K.Dhiman and M.Kumar (2006); Thermal and metal transfer behavior in pulsed current gas metal arc weld deposition of Al-Mg alloy, Science and technology of welding and Joining,vol11(2), pp232-242.

(12) S.G.Sapate, Chakravarthi Gurijala, A.Rathod and A.Singh (2012); Microstructure and abrasive wear properties of Chrome alloy steel, AMAE Int. Journal on Manufacturing and Material Science, vol 02(02), pp 40-43.

(13) E. Farahani, M. Shamanian and F. Ashrafizadeh (2012); A comparative study on direct and pulsed GTAW of alloy 617, AMAE Int. Journal on Manufacturing and Material Science, ©2012 AMAE DOI: 01 JJMMS.02.02.41.

(14) G. A. Roberts, R. Kennedy and G. Krauss, Tool Steels, 5th Edition, ASM International, 2000.

(15) N. Bailey and S. B. Jones (1978); The Solidification cracking of ferritic steel during submerged arc welding, Supplement to Welding Journal, Aug, pp 217-s- 231-s.

(16) J. F. Lancaster (1999), Metallurgy of Welding, Abington Publishing, Woodhead Publishing, Cambridge, England, 6th Edition.